Attenuation Characteristics of Hollow Conducting Elliptical Waveguides

JAN G. KRETZSCHMAR

Abstract—The first-order perturbation formula is used to obtain the attenuation factor of different TE and TM modes in hollow conducting elliptical waveguides. Normalized attenuation charts give the attenuation factor for almost each possible combination of cross-sectional dimensions, nonmagnetic wall material, and frequency of operation.

Introduction

THE first results on the attenuation of different modes in hollow conducting elliptical pipes were given by Chu [1]. In order to simplify the computations known asymptotic expansions were used for the modified Mathieu functions, but this limited the validity of the results. Using the same approach an exact expression for the complex propagation factor was obtained by Piefke [2], but once again a simplification was necessary in order to avoid highly complicated computations. Therefore, new asymptotic formulas, described in [4], were developed by Piefke, but the assumptions made restrict their accuracy in a rather drastic way. Krank [5] used the first-order perturbation method in his analysis, but the deadly slow rate of convergence [8], [13], [14] of the hyperbolic series used to compute the modified Mathieu functions limits the accuracy of his data, especially for the higher order modes (although sufficient accuracy for the dominant mode was obtained).

The purpose of this paper is to present data obtained by using the perturbation method for the analysis and Bessel-function product series for the practical computations of the modified Mathieu functions of the first kind [8], [13], [14]. Furthermore, an approximate formula for the dominant mode, which was proposed by Kihara [6], [7], [10], is verified, and it is shown that the relative error of that formula is smaller than 3 percent over the complete eccentricity and frequency range.

Manuscript received April 23, 1971; revised June 30, 1971. This research was supported by an ESRO-NASA Postdoctoral Fellowship, and was carried out in the Department of Electrical Engineering and Computer Sciences, University of California, Berkeley, Calif.

The author is with the Catholic University of Leuven, Leuven, Belgium.

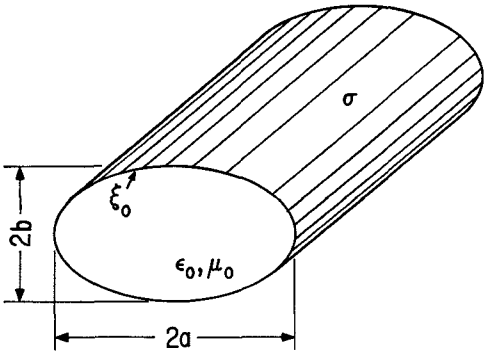

Fig. 1. Hollow conducting waveguide with elliptical cross section.

Attenuation of TE Modes

A harmonic time variation and propagation in the axial direction is assumed for the waves propagating in the hollow conducting elliptical waveguide represented in Fig. 1. When the conducting boundaries have finite conductivity σ, but are still good enough conductors, the attenuation factor α_c due to wall currents can be obtained from the fields in the perfect guide. This procedure is classic and described in most textbooks. The solution for the HSP elliptical guide is well known [1], [11], and using this in the above mentioned method leads to the following normalized expression for the attenuation factor of the even TE_{cm} modes [5] in the guide given in Fig. 1:

$$\alpha_c\sqrt{a^3\sigma} = \left[\frac{\pi\epsilon_0 a f_0}{1-(f_c/f_0)^2}\right]^{1/2} Ce_m^2(\xi_0, q) \cdot \frac{\frac{4q}{e^2}\left(\frac{f_c}{f_0}\right)^2 \int_0^{2\pi} ce_m^2(\eta, q)\sqrt{1-e^2\cos^2\eta}\, d\eta + \left[1-\left(\frac{f_c}{f_0}\right)^2\right]\int_0^{2\pi} \frac{ce_m'^2(\eta, q)}{\sqrt{1-e^2\cos^2\eta}}\, d\eta}{2\int_0^{2\pi}\int_0^{\xi_0} [Ce_m'^2(\xi, q)ce_m^2(\eta, q) + Ce_m^2(\xi, q)ce_m'^2(\eta, q)]\, d\eta\, d\xi} \tag{1}$$

with

$$f_0/f_c = \frac{\pi e}{c\sqrt{q}}(af_0) \tag{2}$$

and

ξ, η	elliptic coordinates,
q	nth nonzero parametric root of $Ce_m'(\xi_0, q) = 0$ (Neumann boundary condition),
$ce_m(\eta, q)$	even Mathieu function of the first kind and order m,
$Ce_m(\xi, q)$	corresponding modified Mathieu function,
f_0	frequency of the wave (Hz),

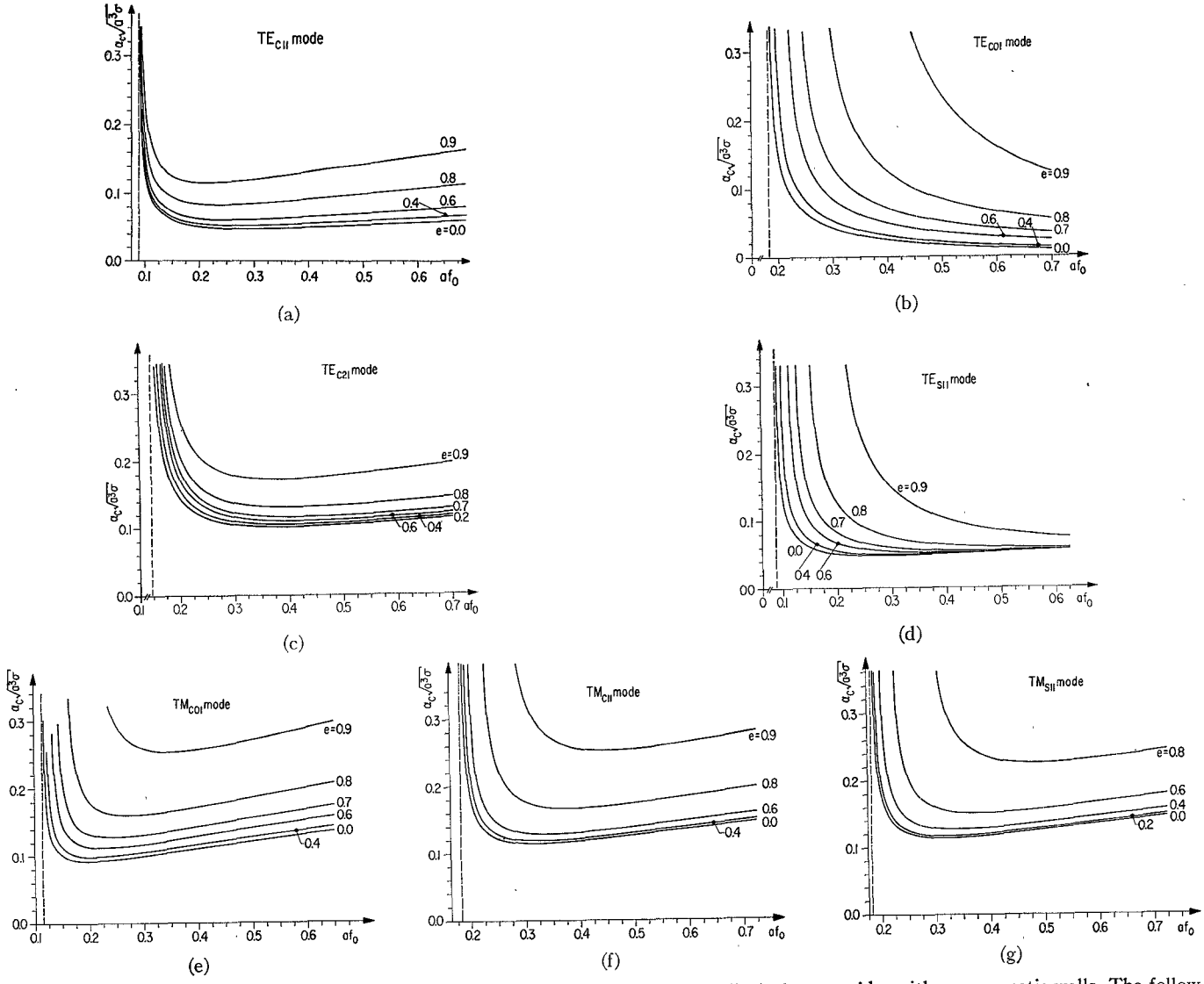

Fig. 2. Normalized attenuation charts for different TE and TM modes in air-filled elliptical waveguides with nonmagnetic walls. The following symbols and units are used: a semimajor axis in meter, e eccentricity of the cross section, α_c attenuation in Np/m, σ conductivity in S/m, and f_0 frequency in GHz.

f_c cutoff frequency of the mnth mode (Hz),
e eccentricity,
ξ_0 radial coordinate of the boundary ellipse,
α_c attenuation factor in Np/m and 1 Np/m = 8.686 dB/m.

The primes in (1) mean the first derivative with respect to the argument ξ or η, as the case may be. The double integral in the denominator of (1) can be reduced to a single one over ξ by applying the properties of the ordinary Mathieu functions [8, sec. 14–40]. The modified Mathieu functions are computed by using Bessel-function product series as described in [8], [13], [14].

With (2) it is obvious that the right-hand side of (1) is a function of the product af_0 and the eccentricity e, and this enables us to construct for each mode a single attenuation chart which gives the attenuation factor for almost each possible combination of σ, f_0, a, and e. The attenuation characteristics obtained for the dominant TE_{c11} mode and the even TE_{c01} mode in an air-filled waveguide with wall conductivity σ are given on Fig. 2(a) and (b). For a given eccentricity the attenuation curves display the same kind of dependence upon the frequency as for the circular case, but for the same mode and the same guidewidth $2a$ the attenuation in the elliptical pipe is always larger than in the circular one, although there is not much difference for small values of e. At a given frequency the attenuation in a guide with a given major axis increases with increasing eccentricity or decreasing minor axis, and this more rapidly as the eccentricity becomes larger. The difference between our results and the curves given by Krank [5] for a TE_{c11} and TE_{c01} mode in a copper guide is small and of the order of the error involved in an interpolation on the charts. This is not the case for results given in [1] and [3]. For a copper elliptical waveguide with eccentricity 0.8 and major axis 3.5 cm an attenuation of 8.3 Np/km at 7 GHz and 6.44 Np/km at 40 GHz is reported in [3] for the dominant mode. For the same guide we obtain 6.53 Np/km and 6.54 Np/km, respectively. Fig. 2(b)

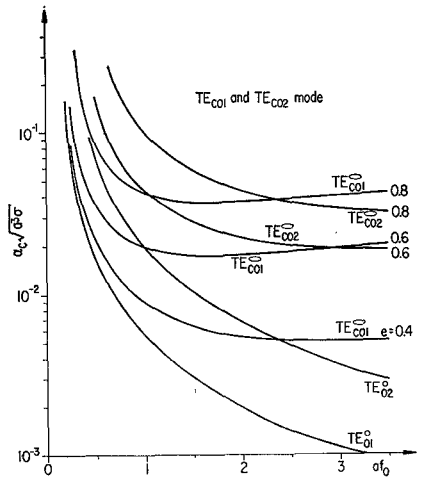

Fig. 3. Normalized attenuation curve of the TE_{c01} and TE_{c02} modes in elliptical guides with different eccentricities.

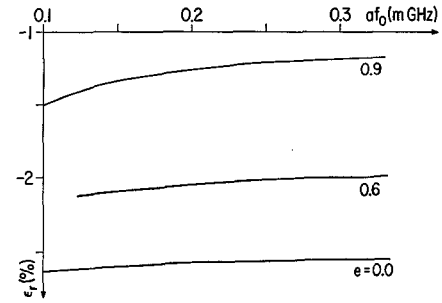

Fig. 4. Relative error of Kihara's approximate formula for the attenuation of the dominant mode in an elliptical waveguide.

suggests that the TE_{c0n} modes have the same anomalous attenuation characteristics as the TE_{0n} modes in circular waveguides. This is true over a large but limited frequency range determined by the eccentricity value. The limitation is due to the fact that the second integral in the numerator of (1) is not zero for TE_{c0n} modes except when $e=0$. For each eccentricity value there is a frequency range where the TE_{c01} mode has the lowest attenuation. Fig. 3 represents the normalized attenuation characteristic of the TE_{01}, TE_{02}, and TE_{c01}, TE_{c02} modes with e as parameter over a broad frequency range. The attenuation of the TE_{c21} mode given on Fig. 2(c) is important too, as this mode becomes the first higher order mode if the eccentricity exceeds about 0.855 [11].

The procedure followed for the odd TE_{smn} modes is exactly the same as for the even ones, and the normalized attenuation factor for the hollow conducting guide is given by (1), except that the even Mathieu and modified Mathieu functions must be replaced by the odd ones.

Fig. 2(d) gives the normalized attenuation chart for the TE_{s11} mode. Over a large interval of frequency the attenuation for a given frequency and major axis increases with eccentricity and does so more rapidly with increasing eccentricity. For higher and higher values of af_0 the attenuation factor tends to an almost eccentricity-independent value, which is approximately equal to the attenuation factor of the TE_{11} mode in the corresponding circular waveguide. Another interesting fact is that for frequencies larger than a certain value (which increases with increasing eccentricity) the attenuation of the odd mode becomes smaller than the attenuation of the dominant even mode. This is completely analogous to the phenomenon that the attenuation of the TE_{01} mode in a rectangular waveguide becomes smaller than the attenuation of the dominant TE_{10} mode in the same guide for frequencies larger than a certain fixed value depending upon the ratio b/a with $b \leq a$.

As the formulas for the attenuation in an elliptical waveguide are quite complicated and require not only the calculation of Mathieu functions, modified Mathieu functions, and their first derivatives, but also of integrals with combinations of those functions as integrand, it is clear that an approximate formula with known accuracy, and not involving those rather uncommon functions, would be very helpful in practical design, especially for the fundamental mode. Using a variational approach, Kihara [6], [10] approximated the electromagnetic field distribution and cutoff wavelength of the dominant mode by algebraic functions. By doing so he obtained an approximate expression for the attenuation factor of the TE_{c11} mode. Normalizing this formula in the same way as was done before gives

$$\alpha_c\sqrt{a^3\sigma} = 0.725F(af_0)^{1/2} \tag{3}$$

and the normalized attenuation factor is once again a function of the product (af_0) and the eccentricity e, as the factor F only depends upon those quantities as explained in [6]. The exact attenuation factor is always smaller than the one given by (3), as the variational approach gives an upper limit for the attenuation factor. Fig. 4 gives the relative error ϵ_r on α_c as a function of (af_0) and e. The frequency f_0 in (3) is in gigahertz.

Attenuation of TM Modes

Using the same approach as for the TE modes one obtains the following expression for the normalized attenuation factor of the even TM_{cmn} modes [5]

$$\alpha_c\sqrt{a^3\sigma} = \left[\frac{\pi\epsilon_0 af_0}{1-(f_c/f_0)^2}\right]^{1/2} \cdot \frac{Ce_m'^2(\xi_0, q)\int_0^{2\pi}\frac{ce_m^2(\eta, q)}{\sqrt{1-e^2\cos^2\eta}}\,d\eta}{2\int_0^{2\pi}\int_0^{\xi_0}\left[Ce_m'^2(\xi, q)ce_m^2(\eta, q) + Ce_m^2(\xi, q)ce_m'^2(\eta, q)\right]d\xi\,d\eta}. \tag{4}$$

The different symbols have the same meaning as before, except for the parameter q. Due to the Dirichlet bound-

ary condition, q is now the nth nonzero parametric zero of the modified Mathieu function of the first kind, order m, and argument ξ_0. Replacing the even Mathieu function in (4) by odd ones gives the attenuation for the odd TM_{smn} modes. Attenuation charts for the TM_{c01}, TM_{c11}, and TM_{s11} modes are given in Fig. 2(e)–(g). Minimum attenuation occurs in the circular guide while the attenuation increases with the eccentricity for a fixed major axis and frequency, and this more rapidly as e becomes larger. The attenuation of the odd TM_{s11} mode is larger than the attenuation of the even TM_{c11} mode, and they do not behave as the even and odd dominant TE_{11} modes. Again, quite a difference between these curves and previously published results [1], [3] is noticed.

Comparison Between Rectangular, Circular, and Elliptical Waveguides with the Same Cutoff Frequency

Although rectangular and some circular guides have standard dimensions and corresponding fixed frequency ranges this is not the case for the less common elliptical guides. This leaves us a wide variety of possibilities for a comparative study. As an example, we compare the WR-90 rectangular guide with a circular and elliptical waveguide with the same cutoff frequency. The rectangular and elliptical guides have the same b/a ratio while all three guides have aluminum walls. Some of their respective properties are summarized in the following table. The attenuation in the elliptical waveguide is approximately 13 percent less than the attenuation in the rectangular guide, while the attenuation of the circular guide is 40 to 50 percent less than the attenuation of the elliptical one. It turns out that in general the attenuation of the dominant mode in an elliptical waveguide is 12 to 15 percent less than the attenuation of the dominant mode in a rectangular guide with the same cutoff frequency, wall material, and side ratio. The circular guide with the same cutoff frequency always has the lowest attenuation of the three types.

Type	Dimensions (cm)	Dominant Mode	f_c (GHz)	First Higher Order Mode	f_c (GHz)
Rectangular (WR 90)	$2a=2.286$ $2b=1.016$	TE_{10}	6.557	TE_{20}	13.114
Elliptical	$2a=2.7304$ $2b=1.2134$	TE_{c11}	6.557	TE_{c21}	12.000
Circular	$2a=2.679$	TE_{11}	6.557	TM_{01}	8.566

Conclusions

The well-known first-order perturbation method applied to elliptical waveguides leads to theoretical formulas for the attenuation due to conductor losses.

The practical application of those formulas not only requires the computation of Mathieu and modified Mathieu functions and their first derivatives, but also requires the evaluation of integrals where the former as well as the latter are involved. Bessel-function product series are quite complicated, especially when differentiation and integration are required, but their high rate of convergence ensures excellent results for the computation of modified Mathieu functions.

Normalization of the attenuation factor for TE and TM modes in hollow conducting pipes with elliptical cross section makes it possible to present for each mode a single attenuation chart for all possible combinations of frequency, eccentricity, major axis, and conductivity of the nonmagnetic metal wall. Applying the same procedure to hollow conducting pipes with rectangular and circular cross section enables an easy comparison of the attenuation characteristics of those three waveguide types. One of the conclusions of such a comparative study is that the attenuation in an elliptical guide is 12 to 15 percent less than the attenuation in a rectangular guide with the same cutoff frequency and axial ratio if both guides operate in their dominant mode. The difference in bandwidth is of the same order, and the rectangular type has the largest bandwidth. This conclusion fits into the more general observation that the elliptical waveguide has some of the advantages as well as some of the disadvantages of both rectangular and circular waveguides.

Although exact computations of the attenuation factor are possible, it is obvious that they are quite cumbersome for practical design purposes. An approximate formula for the dominant mode is therefore verified, and it is shown that its relative error is smaller than 3 percent.

Finally, we can conclude that the results given in this paper, together with the properties described in previous publications, form a fairly complete characterization of hollow conducting elliptical waveguides.

Acknowledgment

The author wishes to thank the members of the Antenna and Propagation group for many helpful discussions and comments. The necessary computations were done on the CDC 6400 computer of the Computer Center at the University of California, Berkeley.

References

[1] L. J. Chu, "Electromagnetic waves in elliptic hollow pipes of metal," *J. Appl. Phys.*, vol. 9, pp. 583–591, Sept. 1938.
[2] G. Piefke, "Grundlagen zur Berechnung der Übertragungseigenschaften elliptischer Wellenleiter," *Arch. Elek. Übertragung*, vol. 18, no. 1, pp. 4–8, 1964.
[3] ——, "Die Übertragungseigenschaften des elliptischen Hohlleiters," *Arch. Elek. Übertragung*, vol. 18, no. 4, pp. 255–267, 1964.
[4] ——, "Asymptotische Näherungen der modifizierten Mathieuschen Funktionen," *Z. Angew. Phys.*, vol. 44, no. 7, 1965.
[5] W. Krank, "Über die Theorie und Technik des elliptischen Wellrohrhohlleiters," dissertation, Rhenish-Westphalian Technical University of Aachen, Aachen, Germany, D 82, 1965.
[6] T. Maeda, "Optimum design dimensions of an elliptical waveguide," *Electron. Commun. Japan*, vol. 51-B, no. 2, pp. 59–63, 1968.
[7] ——, "Design and performance of aluminum elliptical waveguides," *Electron. Commun. Japan*, vol. 51-B, no. 7, pp. 81–88, 1968.
[8] N. W. McLachlan, *Theory and Applications of Mathieu Func-*

tions. New York: Dover, 1964.
[9] NBS, *Tables Relating to Mathieu Functions*. New York: Columbia Univ. Press, 1951.
[10] T. Kihara, *Waveguides*. Tokyo, Japan: Shukyosha Publishers, 1948.
[11] J. G. Kretzschmar, "Wave propagation in hollow conducting elliptical waveguides," *IEEE Trans. Microwave Theory Tech.*, vol. MTT-18, pp. 547–554, Sept. 1970.
[12] ——, "Normalized attenuation charts for rectangular and circular waveguides," to be published.
[13] ——, "Teorie van de gewone en gewijzigde Mathieu funkties van de eerste soort," *Rev. X Tijdschrift*, no. 3, 1969.
[14] ——, "Gewone en gewijzigde Mathieu funkties van de eerste soort. Praktische berekening," *Rev. X Tijdschrift*, no. 4, 1969.
[15] N. Marcuvitz, *Waveguide Handbook*. New York: McGraw-Hill, 1951.

Short Papers

A Novel Design of an *X*-Band High-Power Ferrite Phase Shifter

KARL H. HERING

***Abstract*—A nonreciprocal analog-latching phase-shifter design at *X*-band is described. The device has been operated up to 250 W of average power and 50 kW of peak power. Direct liquid cooling is implemented, pumping FC-78,[1] a dielectric coolant, through the center slot of the ferrite toroid.**

Introduction

A novel design of an *X*-band ferrite phase shifter is presented. The device is designed to handle high power levels—up to 250 W average and 50 kW peak. The phase shifter is of the nonreciprocal analog latching—a name given to the type of digital phase shifters that consist of one long toroidal bar. In this type of device the phase shift is controlled by the driver signal level, as opposed to the conventional digital ferrite phase shifter, which consists of different lengths of ferrite toroids, each driven into saturation. Internal liquid cooling is used to achieve stable performance of the device even at the high average power levels.

The phase shifter required a thermal design of the configuration, selection of the most applicable ferrite material for high-peak and average-power handling, and a method of implementing cooling of the ferrite bar.

Thermal Design Aspects

Applicable methods of cooling the phase-shifter material are: 1) a cold plate [1], 2) forced-air cooling, 3) conduction cooling using boron nitride in contact with the ferrite [2], or 4) direct liquid cooling, as was chosen for this novel phase-shifter design. Other techniques are limited in either cooling potential or for mechanical reasons. Cooling, using a coldplate, has been used successfully in high-power ferrite phase-shifter designs [1], [2]. In doing so, however, the cross section of the phase shifter becomes large. In many phased-array applications very little space is available between the radiating-element/phase-shifter assemblies. Cooling with boron nitride or similar dielectric material of high thermal conductivity reduces phase shift per unit length and provides only limited cooling capability. Forced-air cooling is simple, but provides very limited cooling and precludes that openings exist for the passage of air. Analog phase-shifter designs have shown direct liquid cooling to be far superior to the other techniques. However, the methods used for

Manuscript received March 16, 1970; revised September 7, 1971.
The author was with TRW Corporation, One Space Park, Redondo Beach, Calif. 90278. He is now with the Microwave Division, Aerojet General, Elmonte, Calif. 91734.
[1] Trademark of Minnesota Mining and Manufacturing.

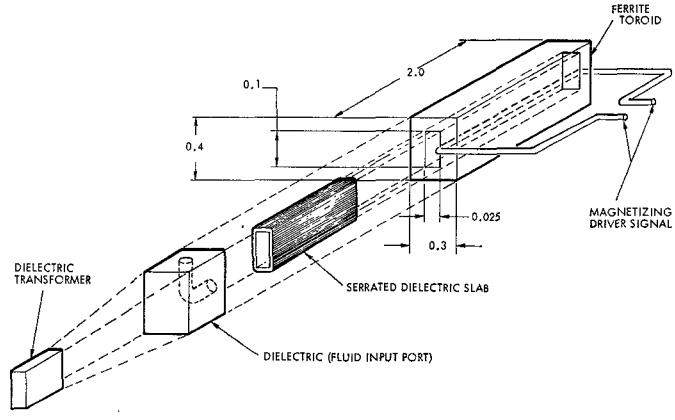

Fig. 1. Direct liquid-cooled *X*-band analog-latching ferrite phase shifter.

S- and *C*-band phase shifters [3] are not applicable at *X* band. In an earlier design for an analog ferrite phase shifter, the bar was encapsulated in a Teflon tube and FC-78[1] was pumped through the device. At *X* band and for a digital ferrite phase shifter this technique is not readily applicable, because of the small size of the ferrite toroid and the drive wire to be brought out through the Teflon tube.

The technique devised and discussed here is shown in Fig. 1. The FC-78 liquid is pumped through inlet/outlet ports into and through the inside of the ferrite toroid. The parts are epoxy bonded to seal the assembly. The inner slot of the ferrite toroid is filled with a serrated dielectric slab, which is a compromise design to allow the liquid to flow through the toroid and to maximize the phase shift. The requirement for the direct liquid-cooling design is determined by calculating the heat load based on the maximum incident RF average power, the insertion loss of the ferrite materials, and the dimensions of the ferrite toroid. The flow rate and the pressure are given by:

$$F_v = \frac{Q}{64.6\ \Delta t} = \text{flow rate (gal/min)}$$

where Q equals the heat load in watts and Δt the temperature rise in degrees, and

$$P = \frac{2.16 \times 10^{-4} f L \rho Q^2}{d^5} = \text{pressure (lbf/in}^2\text{)}$$

where f is the frictional coefficient, ρ is the density of FC-78, L is the length of the toroid, and d is the equivalent diameter of the coolant path through the toroid. The dielectric coolant FC-78 was chosen because of its good thermal and RF characteristics [3].